Anticathode effect on multimodal azimuthal oscillations in electron beam generated $E \times B$ plasma ⊘

Nirbhav Singh Chopra ✉ (iD) ; Yevgeny Raitses (iD)

Check for updates

CHORUS

View Online   Export Citation

Articles You May Be Interested In

Excitation of the modified Simon–Hoh instability in an electron beam produced plasma

Phys. Fluids B (June 1993)

ITEP Bernas ion source with additional electron beam

Rev. Sci. Instrum. (March 2006)

Decaborane beam from ITEP Bernas ion source

Rev. Sci. Instrum. (February 2006)

Anticathode effect on multimodal azimuthal oscillations in electron beam generated E×B plasma

View Online   Export Citation   CrossMark

Nirbhav Singh Chopra[1,2,a)] (iD) and Yevgeny Raitses[1] (iD)

AFFILIATIONS

[1]Princeton Plasma Physics Laboratory, Princeton University, Princeton, New Jersey 08543, USA
[2]Department of Astrophysical Sciences, Princeton University, Princeton, New Jersey 08544, USA

[a)]Author to whom correspondence should be addressed: nschopra@princeton.edu

ABSTRACT

Electron beam (e-beam) generated plasmas with applied crossed electric and magnetic (E × B) fields are promising for low-damage (gentle) material processing. However, these plasmas can be subject to the formation of plasma non-uniformities propagating in the E × B direction. These rotating plasma structures (or "spokes") enhance the transport of charged species across the magnetic field, which can harm the gentle processing capability of the plasma. In this work, we investigate the role of electrostatically active boundaries on the spoke formation by incorporating a variable bias conducting boundary (known as an anticathode) placed on the axially opposite side of the cathode. Our findings indicate azimuthal mode suppression occurs when the anticathode is electron collecting. Furthermore, we show selective azimuthal mode suppression by biasing the anticathode to an intermediate potential between the cathode and anode potentials. These findings suggest a link between the axial electron confinement in the e-beam generated plasma and azimuthally propagating plasma structure formation.

Electron beam (e-beam) generated plasmas with applied electric and magnetic (E × B) fields are promising for applications requiring efficient generation of ions and radicals in low pressure environments.[1–4] A key capability of magnetically confined e-beam plasma sources is that they can generate reactive species while maintaining low energetic particle flux to substrates placed in the periphery of the plasma region.[5–7] However, several operating regimes of cylindrical E × B plasma devices are accompanied by large-scale azimuthally propagating fluctuations in plasma density and potential ("spokes") induced by the modified Simon–Hoh instability (MSHI).[8–11] The spoke has been shown to energize ions in the radial direction, thereby reintroducing energetic ions to the peripheral substrate processing region.[12] Therefore, mitigating the formation of the spoke may enable a wider operating regime of gentle processing capability of the e-beam generated E × B plasma.

Previous work on cylindrical E × B Penning plasma has shown that the axial boundary condition opposite to the cathode plays a major role in the spoke amplitude and frequency by modifying the radial electric field.[8] In particular, it was shown that an electron reflecting floating boundary amplified azimuthal oscillations, while an electron collecting conducting boundary led to azimuthal mode suppression. In this Letter, we experimentally demonstrate the effect of an active axial boundary (the "anticathode") on the formation of azimuthal modes and report on the selective suppression of azimuthal modes using an intermediate anticathode bias. This finding has major implications for a wide range of E × B device applications that simultaneously require high plasma density and mitigation of plasma fluctuations.

The experimental setup consisted of an e-beam generated E × B plasma chamber, which is identical to the setup described in Ref. 13, depicted in Fig. 1(a). An axially mounted thermionic cathode is biased to $V_c = -55$ V and injects an e-beam into the vacuum vessel with a base pressure of $\sim 1\,\mu$Torr, which is then filled with 0.1 mTorr of Ar. The discharge current is $I_d = 100$ mA in all operating regimes considered in this work. The e-beam is injected along the axially applied magnetic field of 100 G produced by a set of axially aligned Helmholtz coils. An anticathode with variable DC bias is installed on the axially opposite side of the chamber. The diagnostic setup is depicted in Fig. 1(b). A Langmuir probe (LP) and emissive probe (EP) diagnostics were used to determine the electron energy distribution function (EEDF), electron density n_e, electron temperature T_e, and plasma potential V_{pl} at different radii. Additionally, an azimuthally oriented
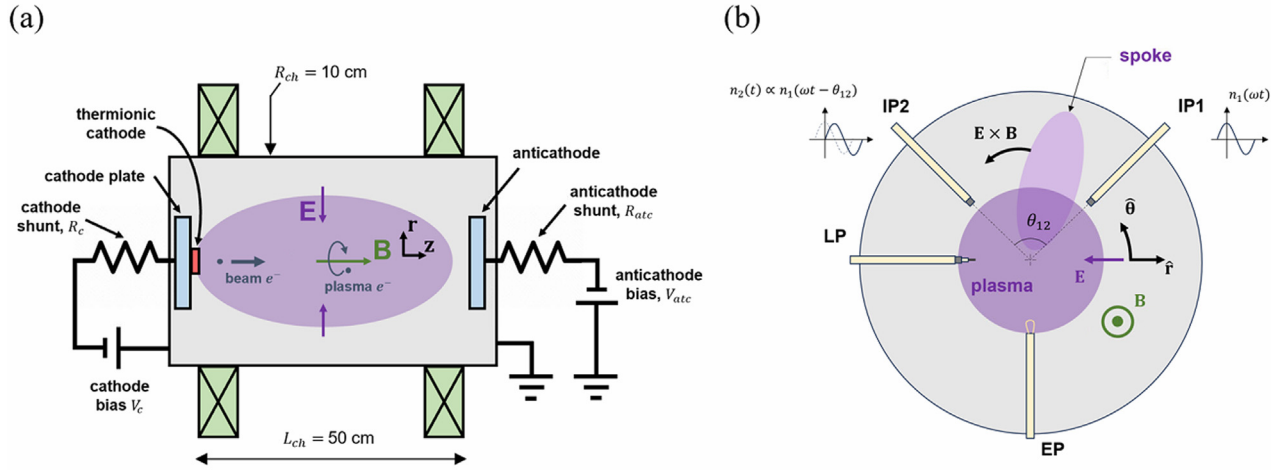
17 February 2025 00:47:22

(a)

(b)

FIG. 1. Schematic of (a) e-beam generated E × B plasma chamber and (b) diagnostic setup.

ion probe (IP) array was used to determine the coherent azimuthally propagating plasma oscillations. The IP array consists of two tungsten wires separated by an azimuthal angle θ_{12}. Each probe wire is negatively biased to −100 V relative to the anode (chamber walls), in which case the ion current collection is in an OML regime.[14,15] A two point-probe correlation technique is used to determine the azimuthally coherent portion of the fluctuating signal collected by each ion probe. The cross power spectral density (CSD) P_{12} is used to quantitatively determine the coherence and relative phase of $n_1(t)$ and $n_2(t)$,[16,17] from which the cross-coherence is defined as[17]

$$C_{12}(f) \equiv \frac{|P_{12}|^2}{|P_{11}||P_{22}|}, \quad (1)$$

where P_{11} and P_{22} are the power spectral densities of n_1 and n_2, respectively. These diagnostics and analysis methods are described in further detail in Refs. 13 and 18.

The results of the measurements are shown in Fig. 2. The radial profiles of electron density and plasma potential are shown in Fig. 2(a), indicating that the Simon–Hoh instability onset criterion is satisfied, $E_r \nabla n_e > 0$.[9,19] The EEDF at $r = 0$ cm determined by LP via the Druyvesteyn method[20] for varying anticathode bias is shown in Fig. 2(b). The depletion of the EEDF can be observed for increasing anticathode bias voltage as the anticathode collects electrons with sufficient energy ε to overcome the anticathode sheath potential drop, $\varepsilon > e(V_{pl} - V_{atc})$.[18]

The Fourier spectra of the plasma density fluctuation measured by IP1 $F(n_1(t))$ at $r = 2.3$ cm for anticathode bias voltages ranging from $V_{atc} = -55$ to 0 V are shown in Fig. 2(c). In the case of electron repelling anticathode with $V_{atc} = -55$ V (repeller mode), there is a prominent low frequency mode occurring at $f_0 = 6$ kHz, an intermediate mode $f_1 = 9$ kHz, and a higher frequency mode $f_2 = 30$ kHz. The above-mentioned oscillations are significantly suppressed when the anticathode is electron collecting $V_{atc} = 0$ V (collector mode) with a significantly weaker mode appearing at $f_c = 15$ kHz.

The cross-coherence $C_{12}(f)$ dependence on the anticathode bias voltage is shown in Fig. 2(d). For $V_{atc} = -55$ V, the azimuthal modes f_0 and f_1 have a high coherence with $C_{12}(f_0) > 0.8$, $C_{12}(f_1) > 0.6$.

Furthermore, f_2 is also azimuthally coherent with $C_{12}(f_2) > 0.2$. The modes f_0 and f_2 obey $\mathrm{Arg}(P_{12}(f_0)) \approx \mathrm{Arg}(P_{12}(f_2)) \approx -\theta_{12}$, indicating that both are single lobed ($m = 1$) modes that are azimuthally propagating in the $+\mathrm{E} \times \mathrm{B}$ direction, which is shown in the supplementary material. Evidently, there is a complex dependence on the anticathode bias on the suppression of the f_0, f_1, and f_2 modes. In particular, intermediate biases between repeller and collector modes at $V_{atc} = -30$ and -15 V selectively suppress f_2 while maintaining the f_0 and f_1 modes. For the electron collecting anticathode case of $V_{atc} = 0$ V, the cross coherence confirms that the azimuthal modes f_0, f_1, and f_2 are suppressed and are replaced by the relatively low coherence azimuthal mode f_c with $C_{12}(f_c) < 0.4$.

In order to understand the trend of azimuthal mode suppression as the anticathode becomes more electron collecting, we apply a one-dimensional electron continuity model to determine the electron transport in the direction perpendicular to the magnetic field. This model is described in greater detail in Refs. 13 and 18 and assumes unmagnetized electrons in the axial direction but magnetized fluid electrons in the radial direction. The drift-diffusion approximation is made for determining the radial electron flux, in which electron transport is determined by an effective cross field mobility and diffusion coefficient. Indeed, for $r > 1$ cm, the EEDF approaches a Maxwellian, which justifies the drift-diffusion approximation for fluid electrons outside of the central e-beam region of the plasma (please see the supplementary material).

As is the case with similar partially magnetized cylindrical E × B plasmas,[8,9,11,12,18] the electron collision rate associated with radial transport is dominated by momentum scattering with plasma fluctuations (so-called anomalous transport). Under these conditions of anomalous cross field electron transport with electron-neutral collision rate much smaller than the anomalous collision rate ($\nu_{en} \ll \alpha\omega_{ce}$), the electron cross field mobility can be approximated as $\mu_{e\perp}(\alpha) \approx \alpha/B$. The anomalous parameter α (inverse Hall parameter) as a function of radial coordinate r is then given by[13]

$$\alpha(r) = B \cdot \frac{\bar{\Gamma}_e^b + \bar{R}_{iz} - \bar{\Gamma}_{e,\mathrm{loss}}^z}{-\left(n_e E_r + \dfrac{\nabla p_e}{e}\right)2\pi r L_{ch}}. \quad (2)$$
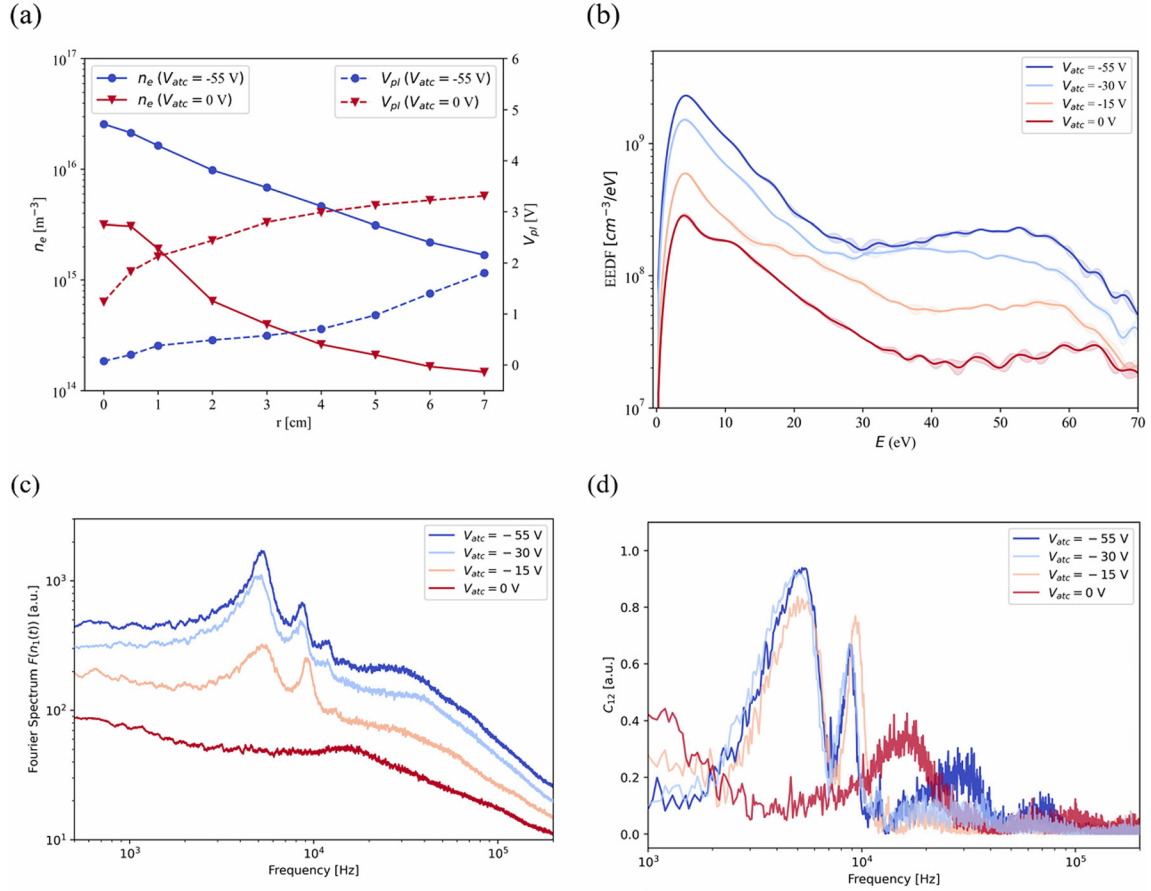
(a)

(b)

(c)

(d)

FIG. 2. (a) Radial profiles of electron density n_e and plasma potential V_{pl}, for anticathode bias voltage $V_{atc} = -55$ V and $V_{atc} = 0$ V. (b) EEDFs determined by LP at $r = 0$ cm for varying anticathode bias voltage V_{atc}, with shaded region indicating the standard deviation of the measured EEDF. (c) Fourier spectra of ion density temporal trace determined by IP for varying values of the anticathode bias voltage V_{atc}; measurements performed at $r = 2.3$ cm. (d) Cross coherence for varying anticathode bias voltage V_{atc}; measurements performed at $r = 2.3$ cm. Parameters are $B = 100$ G, $V_c = 55$ V, and $p = 0.1$ mTorr.

Here, $\bar{\Gamma}^z_{e,loss}$ is the axial electron loss flux integrated over the two cylindrical endcaps of area πr^2, $\bar{\Gamma}^b_e$ is the injected electron beam current, and $\bar{R}_{iz}$ is the ionization rate integrated over the cylindrical volume $\pi r^2 L_{ch}$.[13] Additionally, the numerator in Eq. (2) is proportional to $\bar{\Gamma}^r_e$, the radial electron flux integrated over the cylindrical shell of area $2\pi r L_{ch}$ with corresponding chamber length $L_{ch} = 50$ cm. These integrated quantities are explicitly defined as

$$\bar{\Gamma}^z_{e,loss} = 2\pi \int_0^r r' dr' \frac{n_e v_{the}}{4} \left\{ \exp\left(-\frac{(V_{pl} - V_c)}{kT_e}\right) \right.$$
$$\left. + \min\left[\exp\left(-\frac{(V_{pl} - V_{atc})}{kT_e}\right), 1\right] \right\}, \quad (3)$$

$$\bar{\Gamma}^r_e(\alpha) = -\mu_{e\perp}(\alpha)\left(n_e E_r + \frac{\nabla p_e}{e}\right) \cdot (2\pi L_{ch} r), \quad (4)$$

$$\bar{R}_{iz}(r) = 2\pi L_{ch} \int_0^r r' dr' R_{iz}, \quad (5)$$

and the injected electron beam flux is approximately the discharge current $\bar{\Gamma}^b_e \approx I_d/e$, with $I_d = 100$ mA. Furthermore, the electron

pressure is determined as $p_e = n_e k_b T_e$. All parameters used to calculate Eq. (2) are experimentally determined.

The resulting modeled anomalous parameter $\alpha_{mod.}$ as a function of the radial coordinate is shown for the repeller and collector mode in Fig. 3. In the repeller mode, there is negligible axially conducted current, and so the anomalous radial electron transport enhances to remove electrons from the center of the plasma and maintain a steady state.[13,18] The anomalous parameter $\alpha_{mod.}$ Based on Eq. (2) demonstrates the trend that the anomalous parameter reduces when the anticathode is biased to be electron collecting at $V_{atc} = 0$ V. In this mode, the modeled anomalous factor $\alpha_{mod.}$ reduces to 0 at $r = 2.3$ cm, which coincides with the reduction in azimuthal mode coherence observed experimentally at $r = 2.3$ cm (Fig. 2). This indicates that in the collector mode, the current conduction is constituted by mostly enhanced axial electron loss current to the anticathode, necessitating less anomalous cross field (radial) electron transport to achieve a steady state. This behavior may explain why the azimuthal modes observed with an electron collecting anticathode are significantly less coherent than with an electron repelling anticathode.
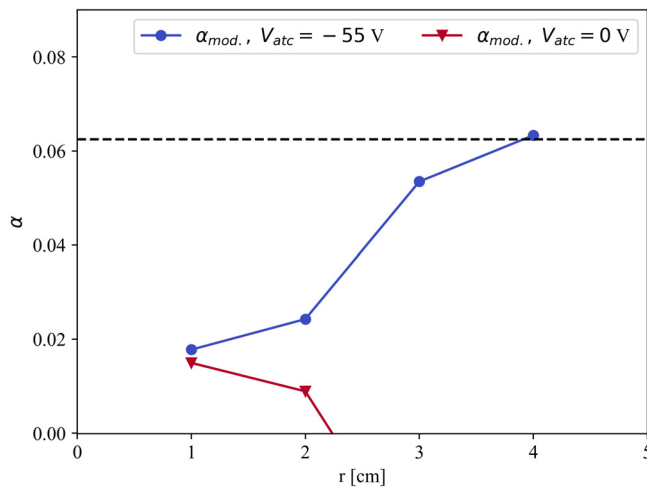
17 February 2025 00:47:22

FIG. 3. Anomalous parameter $\alpha_{mod.}$ as a function of radius, as determined by Eq. (2), for $V_{atc} = -55\,\text{V}$ (blue, repeller mode) and $0\,\text{V}$ (red, collector mode). The value of the anomalous parameter determined by Bohm is indicated by the horizontal dashed line ($\alpha = 1/16$, Ref. 23).

It should be noted that previous works on similar $E \times B$ plasmas (i.e., Hall effect thrusters) have shown that increasing the electron emission current reduces the anomalous cross field electron transport and suppresses low frequency oscillations.[21,22] Future works should investigate the effect of emission current on the anomalous cross field electron transport in the presently studied e-beam generated $E \times B$ plasma.

In summary, biasing the anticathode to be electron repelling sustains at least three azimuthal modes occurring in the 5–50 kHz frequency band, which are likely caused by MSHI, with partial suppression of the azimuthal modes achieved by biasing the anticathode to be electron collecting. The anticathode bias voltage controls the anticathode sheath potential drop, thereby controlling the flux of electrons lost axially. Based on these results, it is suggested that the plasma cannot sustain anomalous radial cross field electron transport when the anticathode is biased to be electron collecting, because of the enhanced axial losses out of the plasma volume at the anticathode sheath. Thus, the biased anticathode can be used to independently control the azimuthal mode formation in axisymmetric e-beam generated $E \times B$ devices. Selective partial mode suppression by applying an intermediate bias shows promise in applications where reduction in plasma oscillations while simultaneously maintaining high bulk plasma density is critical, such as is the case for Hall thrusters for spacecraft propulsion and Bernas ion sources for ion implantation.[24–26]

See the supplementary material for the radial dependence of the measured EEDFs determined by Langmuir probe, as well as the cross coherence and argument of cross spectral density of the ion probe array signals used in this work.

AUTHOR DECLARATIONS
Conflict of Interest

The authors have no conflicts to disclose.

Author Contributions

Nirbhav Singh Chopra: Conceptualization (equal); Data curation (lead); Formal analysis (lead); Investigation (equal); Validation (equal); Writing – original draft (lead); Writing – review & editing (equal). **Yevgeny Raitses:** Conceptualization (equal); Formal analysis (equal); Supervision (lead); Writing – review & editing (equal).

DATA AVAILABILITY

The data that support the findings of this study are available from the corresponding author upon reasonable request.

REFERENCES

[1]F. Zhao, Y. Raitses, X. Yang, A. Tan, and C. G. Tully, "High hydrogen coverage on graphene via low temperature plasma with applied magnetic field," Carbon **177**, 244–251 (2021).

[2]S. G. Walton, D. R. Boris, S. C. Hernández, E. H. Lock, T. Petrova, G. M. Petrov, and R. F. Fernsler, "Electron beam generated plasmas for ultra low T_e processing," ECS J. Solid State Sci. Technol. **4**(6), N5033–N5040 (2015).

[3]D. B. Zolotukhin, V. A. Burdovitsin, and E. M. Oks, "On the role of secondary electrons in beam plasma generation inside a dielectric flask by fore-vacuum plasma-cathode electron source," Phys. Plasmas **24**(9), 093502 (2017).

[4]K. D. Schatz and D. N. Ruzic, "An electron-beam plasma source and geometry for plasma processing," Plasma Sources Sci. Technol. **2**(2), 100–105 (1993).

[5]R. F. Fernsler, W. M. Manheimer, R. A. Meger, J. Mathew, D. P. Murphy, R. E. Pechacek, and J. A. Gregor, "Production of large-area plasmas by electron beams," Phys. Plasmas **5**(5), 2137–2143 (1998).

[6]W. M. Manheimer, R. F. Fernsler, M. Lampe, and R. A. Meger, "Theoretical overview of the large-area plasma processing system (LAPPS)," Plasma Sources Sci. Technol. **9**, 370–386 (2000).

[7]S. Yatom, N. Chopra, S. Kondeti, T. B. Petrova, Y. Raitses, D. R. Boris, M. J. Johnson, and S. G. Walton, "Measurement and reduction of Ar metastable densities by nitrogen admixing in electron beam-generated plasmas," Plasma Sources Sci. Technol. **32**(11), 115005 (2023).

[8]E. Rodríguez, V. Skoutnev, Y. Raitses, A. Powis, I. Kaganovich, and A. Smolyakov, "Boundary-induced effect on the spoke-like activity in $E \times B$ plasma," Phys. Plasmas **26**(5), 053503 (2019).

[9]Y. Sakawa, C. Joshi, P. K. Kaw, F. F. Chen, and V. K. Jain, "Excitation of the modified Simon–Hoh instability in an electron beam produced plasma," Phys. Fluids B: Plasma Phys. **5**(6), 1681–1694 (1993).

[10]J. W. Koo and I. D. Boyd, "Modeling of anomalous electron mobility in Hall thrusters," Phys. Plasmas **13**(3), 033501 (2006).

[11]J. P. Boeuf and M. Takahashi, "New insights into the physics of rotating spokes in partially magnetized $E \times B$ plasmas," Phys. Plasmas **27**(8), 083520 (2020).

[12]M. Tyushev, M. Papahn Zadeh, V. Sharma, M. Sengupta, Y. Raitses, J.-P. Boeuf, and A. Smolyakov, "Azimuthal structures and turbulent transport in Penning discharge," Phys. Plasmas **30**(3), 033506 (2023).

[13]N. S. Chopra, M. P. Zadeh, M. Tyushev, A. Smolyakov, A. Likhanskii, and Y. Raitses, "Multimodal azimuthal oscillations in electron beam generated $E \times B$ plasma," arXiv:2412.01675 (2024).

[14]Y. Raitses, D. Staack, A. Smirnov, and N. J. Fisch, "Space charge saturated sheath regime and electron temperature saturation in Hall thrusters," Phys. Plasmas **12**(7), 073507 (2005).

[15]H. M. Mott-Smith and I. Langmuir, "The theory of collectors in gaseous discharges," Phys. Rev. **28**(4), 727–763 (1926).

[16]P. Welch, "The use of fast fast Fourier transform for the estimation of power spectra: A method based on time averaging over short, modified periodograms," IEEE Trans. Audio Electroacoust. **15**(2), 70–73 (1967).

[17]L. B. White and B. Boashash, "Cross spectral analysis of nonstationary processes," IEEE Trans. Inf. Theory **36**(4), 830–835 (1990).

[18]N. S. Chopra, I. Romadanov, and Y. Raitses, "Anticathode effect on electron kinetics in electron beam generated E × B plasma," Plasma Sources Sci. Technol. **33**(12), 125003 (2024).

[19]A. I. Smolyakov, O. Chapurin, W. Frias, O. Koshkarov, I. Romadanov, T. Tang, M. Umansky, Y. Raitses, I. D. Kaganovich, and V. P. Lakhin, "Fluid theory and simulations of instabilities, turbulent transport and coherent structures in partially-magnetized plasmas of ExB discharges," Plasma Phys. Controlled Fusion **59**(1), 014041 (2017).

[20]M. J. Druyvesteyn, "Der Niedervoltbogen," Z. Phys. **64**(11–12), 781–798 (1930).

[21]Y. Raitses, A. Smirnov, and N. J. Fisch, "Effects of enhanced cathode electron emission on Hall thruster operation," Phys. Plasmas **16**(5), 057106 (2009).

[22]R. Spektor, K. D. Diamant, E. J. Beiting, Y. Raitses, and N. J. Fisch, "Laser induced fluorescence measurements of the cylindrical Hall thruster plume," Phys. Plasmas **17**(9), 093502 (2010).

[23]D. Bohm, E. H. S. Burhop, and H. S. W. Massey, *The Characteristics of Electrical Discharges in Magnetic Fields* (McGraw-Hill, 1949).

[24]M. Farley, P. Rose, and G. Ryding, "Freeman and bernas ion sources," in *The Physics and Technology of Ion Sources*, edited by I. G. Brown (Wiley-VCH Verlag GmbH & Co. KGaA, Weinheim, FRG, 2005), pp. 133–161.

[25]J. Simmonds and Y. Raitses, "Mitigation of breathing oscillations and focusing of the plume in a segmented electrode wall-less Hall thruster," Appl. Phys. Lett. **119**(21), 213501 (2021).

[26]A. Perel, G. Wright, A. McLaughlin, A. Likhanskii, C. Chaney, J. Scheuer, and S. Madunts, "Plasma density oscillations in an ion implanter source and their effect on ion beam transmission," in 77th Annual Gaseous Electronics Conference (2024).

17 February 2025 00:47:22